

Broadband Sub- λ GHz ITO Plasmonic Mach-Zehnder Modulator on Silicon Photonics

Rubab Amin,¹ Rishi Maiti,¹ Yaliang Gui,¹ Can Suer,¹ Mario Miscuglio,¹ Elham Heidari,² Ray T. Chen,² Hamed Dalir,³ and Volker J. Sorger^{1,*}

¹Department of Electrical and Computer Engineering, George Washington University, Washington, DC 20052, USA

²Microelectronics Research Center, Electrical and Computer Engineering Department, University of Texas at Austin, Austin, Texas 78758, USA

³Omega Optics, Inc. 8500 Shoal Creek Blvd., Bldg. 4, Suite 200, Austin, Texas 78757, USA

*Corresponding author: sorger@gwu.edu

Here, we demonstrate a spectrally broadband, GHz-fast Mach-Zehnder interferometric modulator, exhibiting a miniscule $V_{\pi}L$ of 95 V $\cdot\mu\text{m}$, deploying a sub-wavelength short electrostatically tunable plasmonic phase-shifter, based on heterogeneously integrated ITO thin films into silicon photonics.

Indium tin oxide (ITO), belonging to the class of transparent conductive oxides, is a material extensively adopted in high-tech industry such as in touchscreen displays of smartphones or contacts for solar cells. Recently, ITO has been explored for electro-optic modulation using its free-carrier dispersive effect enabling unity-strong index modulation [1-4]. However, GHz-fast modulation capability using ITO is yet to be demonstrated – a feature we show herein. Given the ubiquitous usage of phase-shifter technologies, such as in data communication, optical phased arrays, analog and RF photonics, sensing etc.; here we focus on a Mach-Zehnder interferometer (MZI) based modulator to demonstrate a comprehensive platform of heterogeneous integration of ITO-based opto-electronics into silicon photonic integrated circuits (PIC). Since for phase-shifters only the real-part of the optical refractive index (n) is of interest, in previous studies we have shown the interplay between a selected optical mode (e.g. photonic bulk vs. plasmonic) and the material's figure of merit ($\Delta n/\Delta\alpha$), where α is the optical loss, directly resultant from Kramers-Kronig relations [5]. Additionally, ITO can be selectively prepared (via process conditions [6]) for operating in either an n -dominant or α -dominated region [5]. Using this approach, we recently showed a photonic-mode ITO-oxide-Si MZI on silicon photonics characterized by a $V_{\pi}L = 0.52 \text{ V}\cdot\text{mm}$ [3], and a plasmonic version deploying a lateral gate exhibiting a $V_{\pi}L = 0.063 \text{ V}\cdot\text{mm}$ [7]. Indeed, a plasmonic mode enables a strong light-matter-interaction (e.g. extrinsic slow-light effect), which, when superimposed with ITO's intrinsic slow-light effect, proximal epsilon-near-zero (ENZ) effects [8], enables realization of just 1-5 μm short phase-shifters [5]. The device-advantage of such micrometer-compact opto-electronics are small capacitances, in the order of $\sim\text{fF}$, enabling low power

consumption and small RC delays for fast signal reconfiguration, as shown here. Note, ENZ operation incurs high losses detrimental for phase shifters; as such, the desired operation region is adequately close-to, but not at the high-loss ENZ (ENZ located in α -dominant region) [5]. Here, we discuss an ITO-plasmon-based phase-shifter hetero-geneously integrated into a silicon photonic MZI delivering GHz-fast modulation while being spectrally broadband, thus opening up opportunities for multi-spectral operation. Refraining to exploit feedback from a resonator has several advantages: a) no spectral alignment to the pump laser is required; b) Thus, no heaters are needed for thermal tuning, which would raise the power consumption per-device into the $\sim n$ /bit levels [9]; c) Heat spreads $\sim 100 \mu\text{m}$'s across the PIC, thus packaging density can be significantly improved; d) The photon-lifetime of high- Q cavities can limit RF modulation speed, which is not the case here.

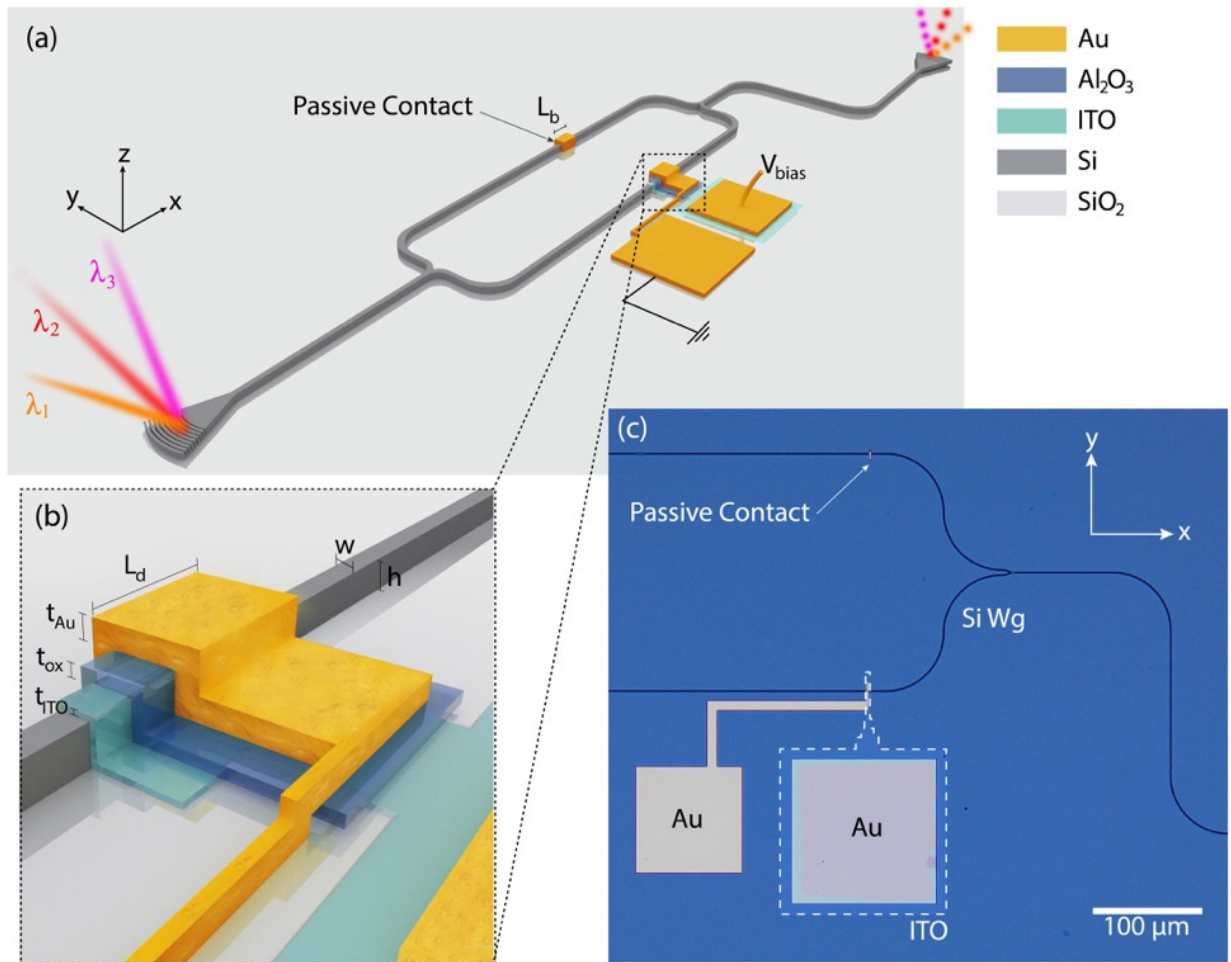


Figure 1. (a) Schematic of the broadband GHz plasmonic ITO-based Mach Zehnder modulator ; (b) Active device region, L_d ; $t_{Au} = 50 \text{ nm}$, $t_{ox} = 20 \text{ nm}$, $t_{ITO} = 10 \text{ nm}$, $w = 500 \text{ nm}$, $h = 220 \text{ nm}$; corresponding FEM eigenmode profiles to light ON and OFF states (inset); (c) Optical microscope image of the sub- λ ($L_d = 1.4 \mu\text{m}$) modulator.

The base interferometer is taped out as a symmetric SOI MZI to minimize chirp effects in modulation induced by different splitting ratios in the Y-junctions of the MZI and includes post-tape out loss-balancing between both arms using a metallic strip (L_b) on the non-modulated arm to minimize extinction ratio (ER) degradation effects (Fig. 1a). Our sweep of the active phase-shifter device length (L_d) ranges from sub- λ (1.4 μm) to λ -scale devices (3.5 μm) [Fig. 1b]. Broadband spectral response is measured in C-band region (~ 30 nm, Fig. 2a); which is expected since the plasmonic resonance of the mode has a FWHM of 100's of nm. The spectral response of the device is determined by ITO dispersion and proximity to ENZ. For ultra-broadband applications (e.g. 100+ nm) ITO modulators for different spectral regions (e.g. $\Delta\lambda = 50$ nm) can be processed using different conditions as demonstrated earlier [6]. Functional capacitor traits in the measured bias range is observed (Fig. 2b). DC electro-optic transmission power tests and squared cosine fit (as dictated by MZI operating principle) result in an ER of ~ 3 dB to >8 dB, respectively (Fig. 2c).

The measured $V_{\pi L}$ is just 95 ± 2 V $\cdot\mu\text{m}$ and found to be rather constant across all device scaling. While these prototype devices require a relatively high voltage ($V_{\pi, \text{as-is}} \sim 26$ V, $\epsilon_{r, \text{Al}_2\text{O}_3} = 11$, $t_{\text{ox}} = 20$ nm), the $V_{\pi, \text{future-option}} = 1$ V can be reached using 5 nm high-k dielectrics (e.g. Hf_3N_4 [10]) in a push-pull configuration. The results indicate a modal index change Δn_{eff} of ~ 0.2 (Fig. 2d) and FEM eigenmode analysis (inset, Fig. 1a) reveals an ITO index change of about 0.6 (Fig. 2e) reflecting an $\sim 2\times$ increased modal confinement factor (Γ) corresponding to active biasing, slightly lower than previous modulators in ITO [3], and intentionally enabling lower insertion loss (IL) of about 6.7 dB. Cutback measurements reveal 1.6 dB/ μm propagation loss in the active capacitive stack and an additional 1.3 dB/coupling loss from in/out coupling of the mode from the Si waveguide, while the passive contact for loss balancing (Fig. 1a, L_b) exhibits a 1.2 dB/ μm propagation loss and 1.1 dB/coupling loss correspondingly. The deposited ITO thin film carrier concentration, N_c of $3.1 \times 10^{20} \text{ cm}^{-3}$ is determined from metrology (e.g. ellipsometry) and a carrier change $\Delta N_c = 2.1 \times 10^{20} \text{ cm}^{-3}$ estimated from the gated measurements places the operation of these devices in the n -dominant operation region, however intentionally away from the high-loss ENZ ($6\text{-}7 \times 10^{20} \text{ cm}^{-3}$) state, yet sufficiently near to capture a slow-light effect [5].

Frequency response (S_{21}) is obtained by generating a low power modulating signal (0 dBm) with a 50 GHz network analyzer; a bias-tee combines DC voltage bias (6 V) with the RF signal (Fig. 2f). RF output from the modulator is amplified using broadband EDFA (~ 35 dB), an optical tunable filter enhances the signal integrity and reduces undesired noise by 20 dB. The modulated light is collected by a photodetector with a single mode fiber. The -3 dB roll-off (small signal) shows a speed of 1.1 GHz (Fig. 2g), which matches estimations for the RC-delay given a capacitance of 213 fF (area = 42 μm^2) and a total resistance of 680 Ω , aligned with our earlier results [3]. A proportionate dynamic switching energy of ~ 21 pJ/bit characterizes the spectral broadband tradeoff in this device. Future improvements such as optimized contact placement, deployment of high-k gate dielectrics including t_{ox} scaling, and utilizing push-pull schemes can enable switching energy reduction of $\sim 10^3\times$, thus only requiring a few fJ/bit. However, aJ/bit energy levels are likely not feasible in non-resonator schemes due to the tradeoff in spectral bandwidth (i.e. no cavity feedback).

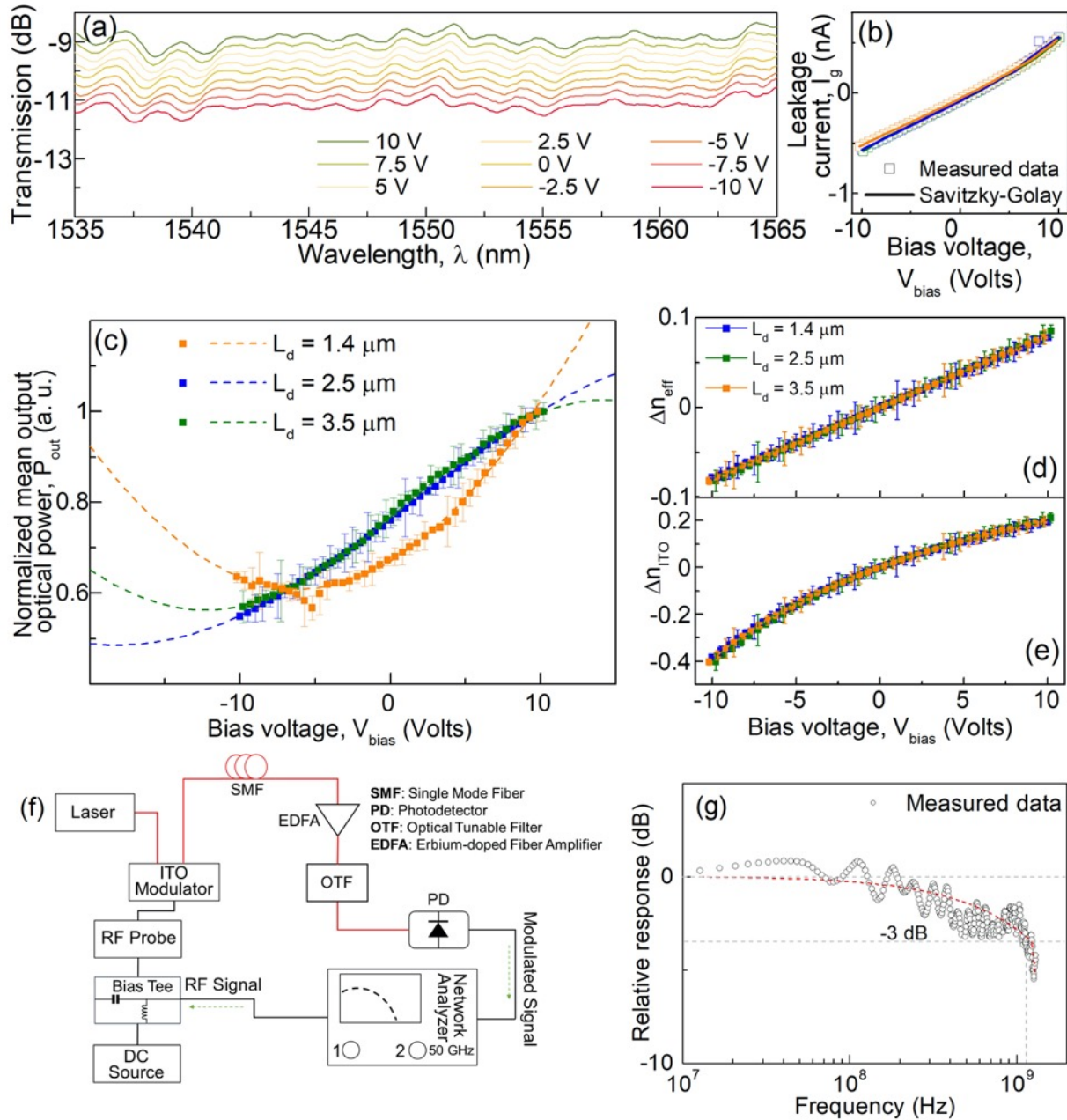


Figure 2. (a) Optical transmission exhibiting broadband performance of the modulator; (b) I-V measurements; (c) Optical output modulation under DC bias for different device scaling, dashed lines are represent $\cos^2(\arg)$ fit dictated by Mach-Zehnder operating principle; (d) Induced effective index change, Δn_{eff} , and (e) ITO material index change, Δn_{ITO} from applied bias; (f) Experimental high-speed set-up; and (g) Measured small-signal response, S_{21} of the modulator establishing a -3 dB bandwidth of 1.1 GHz.

In conclusion, here, we have demonstrated a spectrally broadband, wavelength-compact, GHz-fast ITO-based MZI modulator in silicon photonics showing a low $V_{\pi}L$ of 95 V $\cdot\mu$ m enabled by: a) efficient material modulation in ITO optimized for real-part index operation, b) a plasmonic hybrid mode enhancing the light-matter interaction, c) relatively low electrical resistance, and d) operating away from an optical resonance. This

demonstration bears relevance, since ITO is a foundry-near material with a reduced barrier for co-integration. Future improvements on capacitance, electrostatics, and push-pull designs anticipate a ~ 10 GHz device with a few fJ/bit operation. Next-generation modulators, especially those with near-foundry potential, could be utilized not only in interconnect applications, but also for network-on-chip solutions [11] or more recently as nonlinear activation functions (threshold) in photonic artificial neural networks [12-15] for applications in machine learning. However, for the latter, the optical-electrical-optical conversion at every neuron using the modulator neurons could be improved with respect to signal delay by transitioning to all-optical neural networks [16].

Acknowledgements

Air Force Office of Scientific Research (FA9550-17-1-0071 and FA9550-17-1-0377).

References

1. V. J. Sorger, N. D. Lanzillotti-Kimura, R. Ma, and X. Zhang, "Ultra-compact silicon nanophotonic modulator with broadband response," *Nanophotonics* **1**, 17-22 (2012).
2. A. Melikyan, N. Lindenmann, S. Walheim, P. M. Leufke, S. Ulrich, J. Ye, P. Vincze, H. Hahn, Th. Schimmel, C. Koos, W. Freude, and J. Leuthold, "Surface plasmon polariton absorption modulator," *Optics Express* **19**, 8855-8869 (2011)
3. R. Amin, R. Maiti, C. Carfano, Z. Ma, M.H. Tahersima, Y. Lilach, D. Ratnayake, H. Dalir, and V.J. Sorger, "0.52 V mm ITO-based Mach-Zehnder modulator in silicon photonics," *APL Photonics* **3**, 126104 (2018).
4. E. Li, Q. Gao, S. Liverman, and A. X. Wang, "One-volt silicon photonic crystal nanocavity modulator with indium oxide gate," *Optics Lett.* **43**, 4429-4432 (2018)
5. R. Amin, C. Suer, Z. Ma, I. Sarpkaya, J. B. Khurgin, R. Agarwal, and V. J. Sorger, "Active material, optical mode and cavity impact on nanoscale electro-optic modulation performance," *Nanophotonics* **7**, 455-472 (2017).
6. Y. Gui, M. Miscuglio, Z. Ma, M. H. Tahersima, S. Sun, R. Amin, H. Dalir, and V. J. Sorger, "Towards integrated metatronics: a holistic approach on precise optical and electrical properties of indium tin oxide," *Sci. Rep.* **9**, 11279 (2019).
7. R. Amin, R. Maiti, J. K. George, X. Ma, Z. Ma, H. Dalir, M. Miscuglio, and V. J. Sorger, "A Lateral MOS-Capacitor Enabled ITO Mach-Zehnder Modulator for Beam Steering," *J. Lightwave Technol.* doi: 10.1109/JLT.2019.2956719 (2019).
8. N. Kinsey, and J. B. Khurgin, "Nonlinear epsilon-near-zero materials explained: opinion," *Opt. Mater. Exp.* **9**, 2793-2796 (2019).
9. P. Dong, Y. Chen, G. Duan, and D. T. Neilson, "Silicon photonic devices and integrated circuits," *Nanophotonics* **3**, 215-228 (2014).
10. J.S. Becker, E. Kim, and R. G. Gordon, "Atomic layer deposition of insulating hafnium and zirconium nitrides," *Chem. Mater.* **16**, 3497-3501 (2004).
11. V. K. Narayana, S. Sun, et al. "MorphoNoC: Exploring the Design Space of a Configurable Hybrid NoC using Nanophotonics" *Microprocessors and Microsystems* **50**, 113-126. (2017).
12. M. Miscuglio, G.C. Adam, D. Kuzum, V.J. Sorger "Roadmap on Material-Function Mapping for Photonic-Electronic Hybrid Neural Networks" *APL Materials* **7**, 100903 (2019)

13. R. Amin, R. Maiti, J. K. George, X. Ma, Z. Ma, et al. "A lateral MOS-Capacitor Enabled ITO Mach-Zehnder Modulator for Beam Steering" *Journal Lightwave Technology*, doi: 10.1109/JLT.2019.2956719 (2019).
14. A. Mehrabian, M. Miscuglio, Y. Alkabani, et al. "A Winograd-based Integrated Photonics Accelerator for Convolutional Neural Networks" *IEEE J. of Selected Topics in Quantum Electronics* **26**(1), 1-12 (2019).
15. J. K. George, A. Mehrabian, R. Armin, J. Meng, T. Ferreira De Lima, A. N. Tait, B. Shastri, P. Prucnal, et al. "Noise and Nonlinearity of Electro-optic Activation Functions in Neuromorphic Compute Systems" *Optics Express* **27**, 4 (2019).
16. M. Miscuglio, A. Mehrabian, Z. Hu, S.I. Azzam, J.K. George, A.V. Kildishev, M. Pelton, et al. "All-optical Nonlinear Activation Function for Photonic Neural Networks" *Optical Material Express* **8**(12), 3851-3863 (2018).